Biochemical and Biophysical Research Communications 477 (2016) 834–840

Contents lists available at ScienceDirect

Biochemical and Biophysical Research Communications

journal homepage: www.elsevier.com/locate/ybbrc

The role of receptor topology in the vitamin D3 uptake and Ca^{2+} response systems

Gene A. Morrill*, Adele B. Kostellow, Raj K. Gupta

Department of Physiology and Biophysics, Albert Einstein College of Medicine, Bronx, NY 10461, USA

ARTICLE INFO

Article history:
Received 11 June 2016
Accepted 27 June 2016
Available online 29 June 2016

Keywords:
Vitamin D
VDR
Importin-4
Cholesterol
Transmembrane helices
Calcium channels

ABSTRACT

The steroid hormone, vitamin D_3, regulates gene transcription via at least two receptors and initiates putative rapid response systems at the plasma membrane. The vitamin D receptor (VDR) binds vitamin D_3 and a second receptor, importin-4, imports the VDR-vitamin D_3 complex into the nucleus via nuclear pores. Here we present evidence that the ***Homo sapiens*** VDR homodimer contains two transmembrane (TM) helices ($^{327}E - D^{342}$), two TM "half-helix" ($^{264}K - N^{276}$), one or more large channels, and 16 cholesterol binding (CRAC/CARC) domains. The importin-4 monomer exhibits 3 pore-lining regions ($^{226}E - L^{251}$; $^{768}V - G^{783}$; $^{876}S - A^{891}$) and 16 CRAC/CARC domains. The MEMSAT algorithm indicates that VDR and importin-4 may not be restricted to cytoplasm and nucleus. VDR homodimer TM helix-topology predicts insertion into the plasma membrane, with two 84 residue C-terminal regions being extracellular. Similarly, MEMSAT predicts importin-4 insertion into the plasma membrane with 226 residue extracellular N-terminal regions and 96 residue C-terminal extracellular loops; with the pore-lining regions contributing gated Ca^{2+} channels. The PoreWalker algorithm indicates that, of the 427 residues in each VDR monomer, 91 line the largest channel, including two vitamin D_3 binding sites and residues from both the TM helix and "half-helix". Cholesterol-binding domains also extend into the channel within the ligand binding region. Programmed changes in bound cholesterol may regulate both membrane Ca^{2+} response systems and vitamin D_3 uptake as well as receptor internalization by the endomembrane system culminating in uptake of the vitamin D_3-VDR-importin-4 complex into the nucleus.

1. Introduction

Vitamin D exists as a steroid hormone precursor in two forms: Ergocalciferol (vitamin D_2) which is present in plants and some fish, and Cholecalciferol (vitamin D_3) which is synthesized in the skin from 7-dehydrocholesterol by the ultraviolet B present in sunlight (reviewed in Refs. [1–5]). In vertebrates, a major role of vitamin D is to maintain normal blood levels of calcium and phosphorus. Vitamin D helps the body absorb calcium, which forms and maintains strong bones. It has been used alone or together with calcium to improve bone health and decrease fractures. A vitamin D-binding albumin-like protein transports the newly formed vitamin D to the liver where it undergoes hydroxylation to 25(OH)D (the inactive form of vitamin D) and then to the kidneys where it is hydroxylated to 1,25$(OH)_2$D (the active form). Most of the physiological actions of vitamin D_3 are thought to be exerted through the nuclear vitamin D receptor (VDR) (cit. [2,6,7]). VDR possesses two distinct nuclear transport pathways, i.e. the ligand-dependent and −independent pathways. Importin-4 serves as a nuclear transport receptor and is thought to mediate docking of the importin/substrate complex to the nuclear pore complex [8]. VDR has been shown to influence a variety of physiological functions, affecting nearly every organ and tissue [9]. VDR is one of a large (~1900) number of DNA-binding transcription factors (i.e. proteins that sequence-specifically contact genomic DNA, cit. [10]). VDR has at least three dimerization interfaces: 1) the first zinc finger region, 2) the region just beyond this zinc finger, and 3) the carboxyterminal region [11]. The first zinc finger region (residues 24–44) alone forms a homodimer with full-length VDR. The ligand binding domain of the human VDR has been modeled based on the crystal structure of the retinoic acid receptor [11]. In this study we have examined the topology of the ligand-binding region in the VDR monomer and found evidence for at least one transmembrane

* Corresponding author.
E-mail address: gene.morrill@einstein.yu.edu (G.A. Morrill).

http://dx.doi.org/10.1016/j.bbrc.2016.06.143

Table 1
Summary of regions of *Homo sapiens* vitamin D_3 nuclear hormone receptor.

Regions Accession #P11473	Position of region (amino acid)	Region length residues	Cavity- lining residues
Chain	1–427	427	ND[a]
3D structure database	118–427	309	91
DNA binding region	21–96	75	ND[a]
Hinge region	97–191	94	9
Ligand-binding region	192–427	235	82
Vitamin D3 binding site	227–237	11	5
Vitamin D3 binding site	271–278	8	6
MemBrain (TM half-helix)	263–275	12	10
MemBrain (TM half helix)	328–342	14	9
MEMSAT-SVM (TM helix)	328–343	15	10
CRAC/CARC	240–254	14	5
Domains	313–322	10	3
Ligand-binding	363–370	8	3
Region	399–404	6	4

[a] ND: Not determined.

helix, a large channel structure that traverses the VDR molecule and multiple cholesterol binding sites. In contrast, we find that importin-4 contains 3 pore-lining regions known to be essential in Ca^{2+} uptake as well as 16 additional cholesterol binding sites. This is evidence that the vitamin D_3—importin-4 receptor complex may act both at the plasma membrane as well as through the nuclear vitamin D receptor (VDR)-mediated control of target genes (reviewed in Refs. [2,6]).

2. Material and methods

The amino acid sequences of *Homo sapiens* vitamin D_3 receptor (Accession #P11473) and importin-4 (Accession #Q8TEX9) were obtained from the ExPASy Proteonomic Server of the Swiss Institute of Bioinformatics (http://www.expasy.org; http://www.uniprot.org). As discussed by Nugent and Jones [12], technical difficulties in obtaining high quality crystals have led to an under-representation of channel proteins in structural databases. These workers have trained a support vector machine classifier to predict TM helices (MEMSAT-SVM): (http://bioinfo.cs.ucl.ac.uk/psipred/). Shen and Chou have developed [13] a machine-learning based predictor, MemBrain, that demonstrates an overall improvement in prediction accuracy and classification of transmembrane helices by dynamic threshold: (www.csbio.sjtu.edu.cn/bioinf/MemBrain/). The identification of the largest channel in transmembrane proteins from their crystallographic structure coordinates was carried out using PoreWalker [14]. The PoreWalker web-server is available at http://www.ebi.ac.uk/thorntonsrv/software/PoreWalker/. Two cholesterol recognition domains (CRAC and CARC) have been identified (reviewed in Ref. [15]). The CARC domain is comparable to the CRAC domain but exhibits the opposite orientation ("inverted CRAC").

3. Results

3.1. Transmembrane helices in the vitamin D_3 receptor (VDR)

As outlined in Table 1, ***Homo sapiens*** VDR (Accession #P11473) contain 427 residues. Residues 21–96 have been identified as the DNA binding region, residues 97–191 as a hinge region and 192–427 as the ligand-binding region. Much of the structural analysis of VDR has concerned modeling of the ligand-binding domain and not the total protein. X-ray crystallographic structural data is only available for positions 118–427. The first zinc finger region (residues 24–44) is necessary for formation of a homodimer but is not included in the x-ray analysis. As shown in Fig. 1, computational analysis of the total VDR sequence predicts a 16 residue TM helix ($^{328}E - R^{343}$) within the ligand-binding domain using the MEMSAT-SVM algorithm [12], whereas the MemBrain algorithm [13] predicts possible two half-helic*es* (12 and 14 residues). The second TM helix predicted by MemBrain ($^{328}E - D^{342}$) coincides with the TM helix predicted by MEMSAT. Shen and Chou [13] define a 12-residue sequence as a "half-helix" and note that about 5% of the TM helices in known structures are very short (<15 residues) and some may only span the membrane partially.

Analysis of 160 TM helices of 15 non-homologous high-resolution X-ray protein structures by Hildebrand et al. [16] indicate that the average length of helices that span the hydrophobic part of the bilayer is 17.3 ± 3.1. Algorithms such as TMHMM do not detect TM helices shorter than 16 residues whereas the TOPCONS method assumes all TM helices contain 20 residues (cit. [13]). The SVM (support vector machine-based) predictor used in Fig. 1 achieves a topology prediction accuracy of 89% with a low false negative rate of 0.4% [12]. The MemBrain approach integrates a number of bioinformatics approaches including sequence representation by multiple sequence alignment matrixes, the optimized evidence-theoretic K-nearest neighbor prediction algorithm, fusion of multiple prediction window sizes, and classification by dynamic threshold. MemBrain demonstrates overall high prediction accuracy, particularly in TM helices shorter than 15 residues [13]. In contrast, TMHMM and Phobius did not predict TM helices when applied to the VDR dataset. The protein prediction success rate (Vp) is defined as the fraction of helical proteins in the data set that are correctly predicted [17]. Vp for MemBrain was found to be 87.1% compared to 65.7% for TMHMM and 71.4% for Phobius.

In the cell, protein synthesis is initiated universally with the amino acid methionine which is subsequently removed by endoproteases (see Ref. [18]). Since x-ray crystallography methods require large quantities of a pure protein [19,20], crystallography "pdb" files of cell-free preparations such as those analyzed by PoreWalker (Fig. 3) contain N-terminal methionine. The codon initiator methionine is therefore listed in Fig. 1, although it may not be present physiologically. A contribution by N-terminal methionine to the crystallographic structure has not been evaluated.

3.2. Cholesterol-binding (CRAC/CARC) domains

Fig. 2 illustrates the amino acid sequence of Homo ***sapiens*** VDR. The MEMSAT-SVM TM helix ($^{328}H - D^{343}$) and the MemBrain "half-helix" ($^{263}L - S^{275}$) are underlined in bold and double-underlined, respectively. In addition to transmembrane helices, functional protein domains such as cholesterol binding CRAC or CARC sequences [15] can also be identified within the VDR sequence and are highlighted in red. CRAC is a short linear amino acid domain

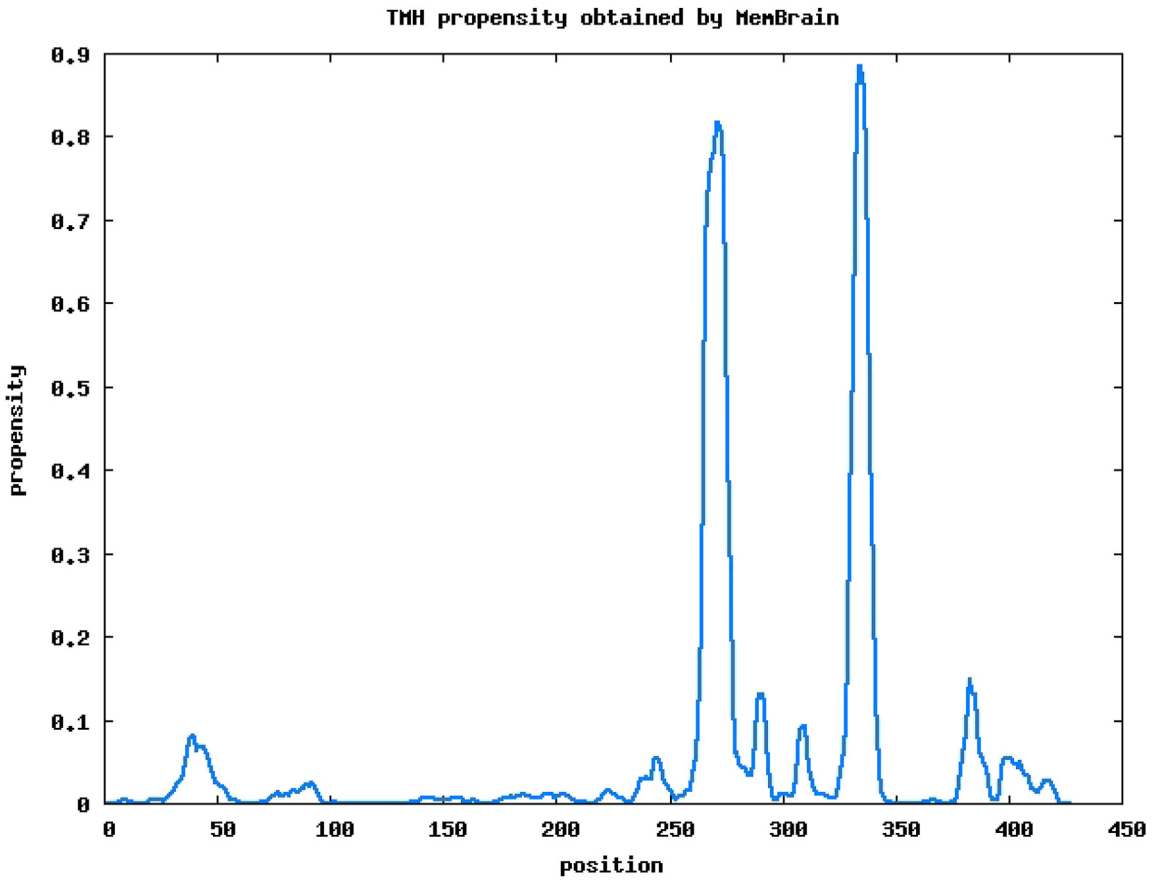

MemBrain Propensity

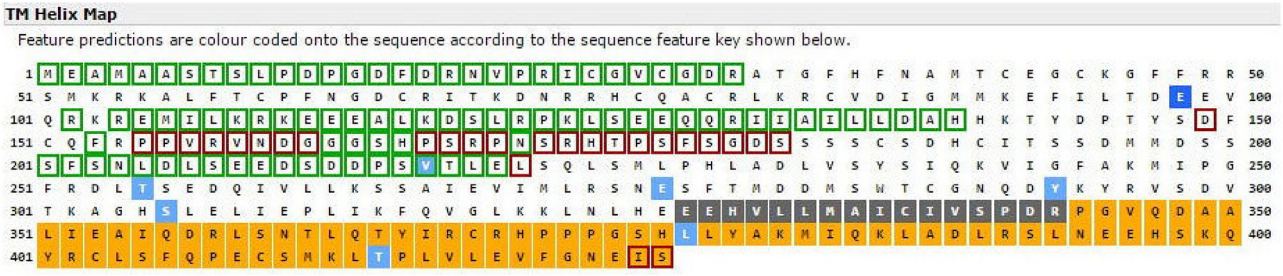

MEMSAT MAP

Fig. 1. Comparison of the topology of *Homo sapiens* Vitamin D_3 Receptor (Accession #P11473) using the MemBrain algorithm (upper plot) and the support vector machine-based TM topology predictor MEMSAT-SVM (lower plot). The transmembrane region for MEMSAT-SVM is highlighted in black. White sequences indicate predicted cytoplasmic regions; those highlighted in orange represent extracellular regions. See Methods for details. (For interpretation of the references to colour in this figure legend, the reader is referred to the web version of this article.)

that mediates binding to cholesterol and stands for **C**holesterol **R**ecognition/Interaction **A**mino acid **C**onsensus sequence. An inverse cholesterol binding domain has also been characterized and is termed a "CARC" domain. As shown, the VDR monomer contains 8 CARC/CARC domains (2 being contiguous; $^{242}V - L^{254}$). The ligand binding domain (residues 192–427 in Fig. 2) contains 4 of the 8 total CRAC/CARC domains. For comparison, the vitamin D_3 binding regions are highlighted in blue ($L–S^{237}$; $^{271}I–S^{288}$). As shown, the second vitamin D_3 binding region ($^{271}I–S^{288}$) overlaps the MemBrain defined "half-helix" ($^{262}L - S^{275}$).

```
          10         20         30         40         50
MEAMAASTSL PDPGDFDRNV PRICGVCGDR ATGFHFNAMT CEGCKGFFRR
          60         70         80         90        100
SMKRKALFTC PFNGDCRITK DNRRHCQACR LKRCVDIGMM KEFILTDEEV
         110        120        130        140        150
QRKREMILKR KEEEALKDSL RPKLSEEQQR IIAILLDAHH KTYDPTYSDF
         160        170        180        190        200
CQFRPPVRVN DGGGSHPSRP NSRHTPSFSG DSSSSCSDHC ITSSDMMDSS
         210        220        230        240        250
SFSNLDLSEE DSDDPSVTLE LSQLSMLPHL ADLVSYSIQK VIGFAKMIPG
         260        270        280        290        300
FRDLTSEDQI VLLKSSAIEV IMLRSNESFT MDDMSWTCGN QDYKYRVSDV
         310        320        330        340        350
TKAGHSLELI EPLIKFQVGL KKLNLHEEEH VLLMAICIVS PDRPGVQDAA
         360        370        380        390        400
LIEAIQDRLS NTLQTYIRCR HPPPGSHLLY AKMIQKLADL RSLNEEHSKQ
         410        420
YRCLSFQPEC SMKLTPLVLE VFGNEIS
```

Fig. 2. Analysis of the amino acid sequence of ***Homo sapiens*** vitamin D_3 receptor (Accession #P11473) for TM helices, vitamin D_3 binding regions and/or protein domains. The TM helix predicted by MEMSAT is single underlined whereas those predicted by the MemBrain algorithm are double underlined. Cholesterol-binding (CRAC/CARC) domains are indicated in red. Vitamin D_3 binding regions are highlighted in blue. For details see Methods. (For interpretation of the references to colour in this figure legend, the reader is referred to the web version of this article.)

3.3. Pore-lining regions in Homo sapiens Importin-4

Importin- 4 (Accession #Q8TEX9) is proposed to function in the nuclear protein import system as a nuclear transport receptor and is thought to mediate docking of the importin/substrate complex to the nuclear pore complex [21]. Nucleoporin and the VDR substrate complex are subsequently translocated through the nuclear pore by an energy-requiring Ran-dependent mechanism (reviewed in Ref. [8]). As shown in Fig. 3, computational analysis of the total importin-4 sequence predicts 3 pore-lining regions: a 25 residue pore-lining region ($^{227}A-E^{252}$) and 15 ($^{769}M-T^{784}$) and 16 ($^{877}F-A^{893}$) residue pore-lining sequences within the ligand-binding domain using the MEMSAT algorithm [12].

Pore-lining regions form bundles central to the function of all ion channels and their conformational rearrangements dictate channel gating [21]. The importin-4 monomer contains at least 16 cholesterol (CRAC/CARC) domains, two of which overlap two of the three pore-lining regions. The MEMSAT-SVM MAP represents the topology of the protein involved in partitioning across the plasma membrane, or alternatively, across the nuclear plug. In the latter case, the orange residues indicate cytoplasmic regions whereas the white residues are nucleoplasmic. Fig. 3 predicts that a large 500 plus residue loop (^{225}K to V^{769}) extends into the nucleoplasm. MEMSAT also suggests that importin-4 may insert into the plasma membrane with the N-terminal 224 residues of the ligand-binding region and a 107 residue loop in the C-terminal ligand region being extracellular.

3.4. Characterization of channels and/or pores

Pellegrini-Calace et al. [13] have developed an improved computational approach (PoreWalker 1.0) for the identification and characterization of channels in transmembrane proteins based on their three-dimensional structure. Given a set of 3D crystallography coordinates, this method can detect and identify the pore centers and axis using geometric criteria, identifying the biggest and longest cavity/channel through the protein. Typically, channel proteins contain a cavity (or pore) which spans the entire membrane protein with an opening on each side of the membrane. Pore features, including diameter profiles, pore-lining residues, the size, shape and regularity of the pore are used to provide a quantitative and visual characterization of the channel. However, it should be noted that: 1) the crystals represent only a single low energy state under the crystallization conditions, and 2) crystallization of integral membrane proteins involves removal of bound lipids such as cholesterol (rev. [15]). Since pore-forming proteins interact with lipid bilayers to generate 'proteolipidic' pores [22], the "crystal structure" of the membrane protein may not reflect the physiological cavity/channel.

Fig. 4 illustrates and compares the PoreWalker output for the VDR ligand binding domain (LBD) complexed to vitamin D_3 (1DB1) and identifies and characterizes the biggest and longest channel. 1DB1 is the 1.8 Å resolution crystal structure of the complex between D_3 and a VDR LBD (residues 118–427) lacking the highly variable insertion domain. The crystallographic data indicates that the truncated VDR molecule forms monomers, not the dimer reported for the complete VDR structure [10]. The upper graph illustrates the pore diameter profile, the middle is an image of the cavity, and the lower structure features of the cavity. The protein structure is colored in green. The red spheres represent pore centers at given pore heights and their diameters are proportional to the pore diameter calculated at that point. The section in the lower image was obtained by cutting the protein structure along the XY plane. The upper and middle images indicate a cavity in the C-terminal region of the VDR. The lowest coordinate along the x-axis is at the bottom and illustrates the respective pore in the XY-plane section, $Z > 0$ coordinates only. As can be seen, a channel extends across the LBD and may correspond to the Ca^{2+} and/or phosphate channel.

The PoreWalker method identifies the residues lining the cavity or channel. As shown in Table 1, 15 of the 38 residues associated with the CARC/CARC domains as well as 11 of the 19 residues associated with vitamin D binding are cavity lining residues. Similarly, 29 of the 42 residues associated with both TM helix and "half -helix" structures also line the channel/cavity. Thus 55 of the 82 channel residues estimated to line the ligand-binding region are contributed by vitamin D binding sites, cholesterol binding sites, and both TM helices and "half-helices". As summarized in Table 1, 11 of 19 D_3 binding residues line the channel, whereas 10 of 12 half-helix residues detected by MemBrain and 10 of 16 residues

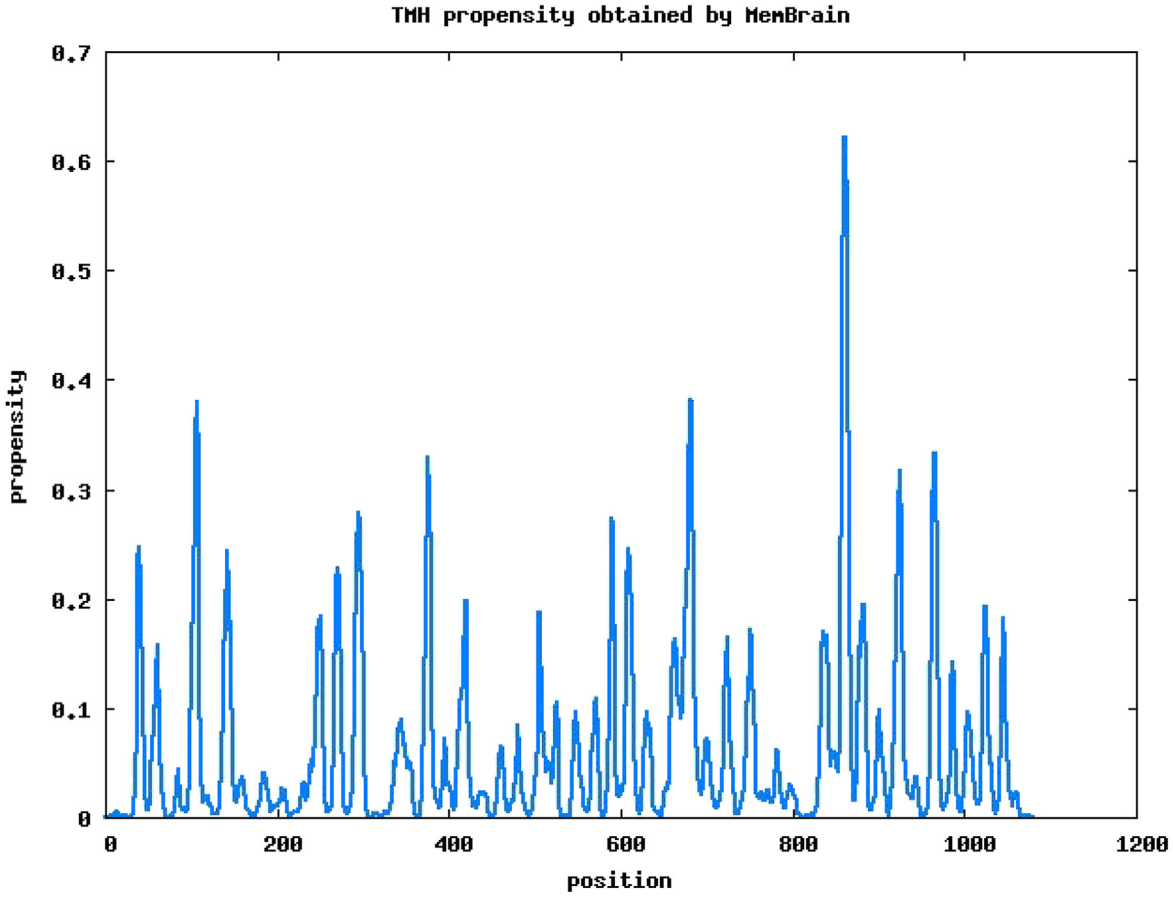

Fig. 3. Comparison of the topology of *Homo sapiens* importin-4 (Accession #Q8TEX9) using the MemBrain algorithm (upper plot) and the support vector machine-based TM topology predictor MEMSAT-SVM (lower plot). The pore-lining regions are highlighted in blue (lower plot). White sequences indicate predicted cytoplasmic regions; those highlighted in orange represent extracellular regions. See Methods for details. (For interpretation of the references to colour in this figure legend, the reader is referred to the web version of this article.)

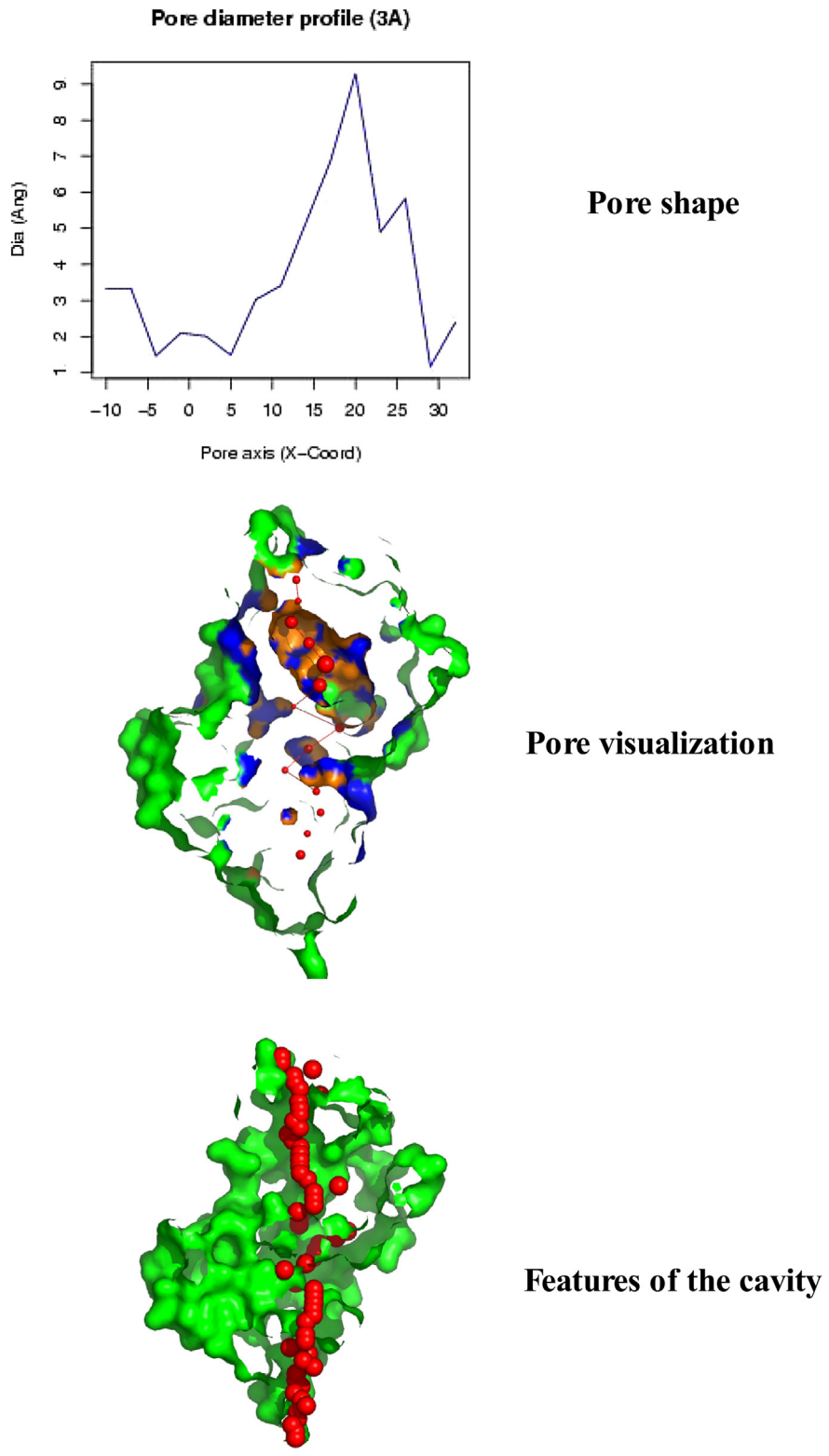

Fig. 4. A comparison of the pore shape profile at 3Å (upper plot), pore visualization cross section (middle plot), and features of the cavity (lower plot) based on a PoreWalker analysis of the crystal structure of VDR ligand binding domain at 1.8 Å (1DB1, residues 118–427). The first zinc finger region (residues 24–44) required to form a homodimer is missing. For details of PoreWalker analysis see Methods.

of the TM helix detected by MEMSAT-SVM are contributed to the channel. As also shown, 15 residues are contributed by the CRAC/CARC domains, indicating that all 4 cholesterol-binding domains play an important role in movement of ions through channels.

4. Discussion

Table 1 summarizes the positions, lengths and number of pore-lining residues associated with the major channel identified within

the ***Homo sapiens*** vitamin D_3 receptor (VDR) molecule. Of the 91 cavity lining residues predicted by PoreWalker (Fig. 4) in the 118–427 residue 3D structure, 19 were associated with the two vitamin D_3 binding sites and 75 with the pore-lining residues of the ligand binding region. Ten cavity-lining residues were contributed by the TM helix identified by MEMSAT-SVM algorithm and another 10 residues were within half-helices identified by the MemBrain algorithm (Fig. 1). Clusters of 38 contact points are contributed by the 4 cholesterol (CRAC/CARC domains) binding sites lining the cavity/channel.

It is important to recognize that the plasma membrane system described here is largely concerned with "cytoplasmic" uptake of vitamin D_3 and Ca^{2+} that in turn leads to nuclear uptake of the D_3-VDR complex by importin-4 [20]. Uptake of the D_3-VDR-importin-4 complex culminates in D_3 regulation of gene transcription. It should be noted that uptake of Ca^{2+} ions is also linked to the VDR-D_3 complex [23], and that pore-lining regions such as those in importin-4 are central to the function of all ion channels [20]. The VDR-D_3-importin-4 complex may regulate Ca^{2+} and PO_4 uptake by cells including osteoblasts. MEMSAT topology of VDR indicates that the D_3-VDR complex may be inserted into the plasma membrane, with the N-terminal 326 residues of the ligand-binding region being extracellular (Fig. 1). The N-terminal 126 residues contain vitamin D_3 binding sites and serve as an uptake route for vitamin D_3 into the cytoplasm via the endomembrane system [24]. Similarly, MEMSAT predicts 3 pore-lining regions in importin-4; one 26 residue and two 16 residue pore-lining regions. Each VDR-importin-4 heterotetramer would thus involve 6 pore-lining regions. As noted by Dai and Zhou [25], the pore-lining regions are central to the function of all ion channels, and may be a key to Ca^{2+} and PO_4^- movement in vitamin D_3-dependent systems. Lippincott-Schwartz and Phair [24] have discussed how membrane lipids and cholesterol may act as regulators of traffic in the endomembrane system.

As shown by Nishikawa et al. [25], VDR exists as a homodimer. Fig. 1 indicates that the VDR homodimer may contain a total of 2 TM helices and 2 half-helices, which would constitute a total of 58 channel lining residues (Table 1). The TM helices and half-helices within the homodimer may merge, under certain physiological conditions, to form a channel as predicted by Hildebrand et al. [16]. Four vitamin D_3 binding sites, within the homodimer, also line the channel indicating that the channels serve both as vitamin D_3 uptake pathways and as calcium conduits. Levitan et al. [26] suggest that cholesterol interacts primarily with hydrophobic residues in the non-annular regions of the channels embedded between TM helices. Based on the Levitan model, multiple cholesterol binding sites within the ligand binding domain are associated with the major channel and regulate the ion channels by altering the physical properties of the lipid bilayer, which in turn affects protein function. As described here, vitamin D is both synthesized from cholesterol and utilizes cholesterol in its receptor-response system. Our finding that cholesterol may be essential for vitamin D receptor function suggests that clinical regimens lowering or depleting cholesterol should be reconsidered.

Conflicts of interest

The authors declare no conflict of interest.

Acknowledgements

This research was supported in part by National Institutes of Health research grants HD10463 and GM-071324.

References

[1] M.R. Haussler, G.K. Whitfield, C.A. Haussler, J.-C. Hsieh, P.D. Thompson, S.H. Selznick, C.E. Dominguez, P.W. Jurutka, The nuclear vitamin D receptor: biological and molecular regulatory properties revealed, J. Bone Min. Res. 13 (1998) 325–349.
[2] S. Kato, The function of vitamin D receptor in vitamin D action, J. Biochem. 127 (2000) 717–722.
[3] S. Yamada, M. Shimizu, K. Yamamoto, Structure-function relationships of vitamin D including ligand recognition by vitamin D receptor, Med. Res. Rev. 23 (2003) 89–115.
[4] R. Khanal, I. Nemere, Membrane receptors for vitamin D metabolites, Crit. Rev. Eukaryot. Gene Expr. 17 (2007) 31–47.
[5] F.C. Campbell, Xu Haibo, M. El-Tanani, P. Crowe, V. Bingham, The Yin and Yang of vitamin D receptor (VDR) signaling in neoplastic progression: operational networks and tissue-specific growth control, Biochem. Pharmacol. 79 (2010) 1–9.
[6] A. Norman, Minireview: vitamin D Receptor: new assignments for an already busy receptor, Endocrinology 147 (2006) 5542–5548.
[7] C. Carlberg, M.J. Campbell, Vitamin D receptor signaling mechanisms: integrated actions of a well-defined transcription factor, Steroids 78 (2013) 127–136.
[8] Y. Miyauchi, T. Michigami, N. Sakaguchi, Y. Yoneda, J.W. Pike, M. Yamagata, K. Ozono, Importin 4 is responsible for ligand-independent nuclear translocation of vitamin D receptor, J. Biol. Chem. 280 (2005) 40901–40908.
[9] Holick M.F, Evolution and function of vitamin D, Recent Results Cancer Res. 164 (2003) 3–28.
[10] G.K. Whitfield, H.T. Dang, S.F. Schuter, R.M. Bernstein, T. Bunag, L.A. Manzon, G. Hsieh, C.E. Dominguez, J.H. Youson, M.R. Haussier, J.J. Marchalonis, Cloning of a functional vitamin D receptor from the lamprey (Petromyzon marinus), an ancient vertebrate lacking a calcified skeleton and teeth, Endocrinology 144 (2003) 2704–2716.
[11] E.J. Reschly, M.D. Krasowski, Evolution and function of the NR1I nuclear hormone receptor subfamily (VDR, PXR, and CAR) with respect to metabolism of xenobiotics and endogenous compounds, Curr. Drug Metab. 7 (2006) 349–365.
[12] T. Nugent, D.T. Jones, Transmembrane protein topology prediction using support vector machines, BMC Bioinform. 10 (2009) 159–170.
[13] H. Shen, J.J. Chou, MemBrain: improving the accuracy of predicting transmembrane helices, PLoS One 3 (2008) e2399.
[14] M. Pellegrini-Calace, T. Malwald, J.M. Thornton, Porewalker: a novel tool for the identification and characterization of channels in transmembrane proteins from their three-dimensional structure, PLoS Comput. Biol. 5 (2009) e1000440.
[15] J. Fantini, F.J. Barrantes, How cholesterol interacts with membrane proteins: an exploration of cholesterol-binding sites including CRAC, CARC, and tilted domains, Front. Physiol. 4 (2013) 31, 28.
[16] P.W. Hildebrand, R. Preisser, C. Frommel, Structural features of transmembrane helices, FEBS Lett. 559 (2004) 145–151.
[17] J.M. Cuthbertson, D.A. Doyle, M.S. Sansom, Transmembrane helix prediction: a comparative evaluation ans analysis, Protein Eng. Des. Sel. 18 (2005) 295–308.
[18] C.C. Valley, A. Cembran, J.D. Perlmutter, A.K. Lewis, N.P. Labello, J. Gao, J.N. Sachs, The methionine-aromatic motif plays a unique role in stabilizing protein structure, J. Biol. Chem. 287 (2012) 34979–34991.
[19] E.P. Carpenter, K. Beis, A.D. Cameron, S. Twata, Overcoming the challenges of membrane protein crystallography, Curr. Opin. Struct. Biol. 18 (2008) 581–586.
[20] M. Watanabe, K. Miyazono, M. Tanokura, T. Sawasaki, Y. Endo, I. Kobayashi, Cell-free protein synthesis for structure determination by x-ray crystallography, Methods Mol. Biol. 607 (2010) 149–160.
[21] J. Dai, H.-K. Zhou, General rules for the arrangements and gating motions of pore-lining helices in homomeric ion channels, Nat. Commun. 5 (2014) 4641, http://dx.doi.org/10.1036/ncomms5641.
[22] R.J. Gilbert, D. Dalla Serra, C.J. Froelich, M.I. Wallace, G. Anderluh, Membrane pore formation at protein-lipid interfaces, Trends Biochem. Sci. 39 (2014) 510–516.
[23] L.P. Zanello, A. Norman, 1alpha, 25(OH)2 vitamin D3 actions on ion channels in osteoblasts, Steroids 71 (2006) 291–297.
[24] J. Lippincott-Schwartz, R.D. Phair, Lipids and cholesterol as regulators of traffic in the endomembrane system, Annu. Rev. Biophys. 39 (2010) 559–578.
[25] J. Nishikawa, M. Kitaura, M. Imagawa, T. Nishihara, Vitamin D receptor contains multiple dimerization interfaces that are functionally different, Nucleic Acids Res. 25 (1995) 606–611.
[26] I. Levitan, D.K. Singh, A. Rosenhouse-Dantsker, Cholesterol binding to ion channels, Front. Physiol. 26 (2014) 65.